

## Icosahedral ordering in liquid iron studied via x-ray scattering and Monte Carlo simulations

Masanori Inui,<sup>1</sup> Kenji Maruyama,<sup>2</sup> Yukio Kajihara,<sup>1</sup> and Masaru Nakada<sup>2</sup>

<sup>1</sup>Graduate School of Integrated Arts and Sciences, Hiroshima University, Higashi-Hiroshima, Hiroshima 739-8521, Japan

<sup>2</sup>Graduate School of Science and Technology, Niigata University, Niigata 950-2181, Japan

(Received 27 February 2009; revised manuscript received 10 August 2009; published 5 November 2009)

X-ray diffraction measurements were carried out for liquid iron near the melting temperature and atomic configurations were constructed from the structure factor  $S(Q)$  obtained, by reverse Monte Carlo modeling and Monte Carlo simulation with the effective pair potential deduced by the inverse method. The bond-orientational order parameter  $\hat{W}_6$  calculated from the atomic configurations obtained from both simulations indicates a pronounced icosahedral ordering, and the fraction of nearly icosahedral configurations is estimated to be approximately 14% in liquid iron. These experimentally obtained results seem consistent with recent results of *ab initio* molecular-dynamics simulation for liquid iron [P. Ganesh and M. Widom, Phys. Rev. B **77**, 014205 (2008)].

DOI: 10.1103/PhysRevB.80.180201

PACS number(s): 61.25.Mv, 61.05.C-, 61.20.Ja

Liquid levitation without using any container has become a useful method for studying structural and physical properties in the liquid state, particularly for materials with high melting temperatures. Although the diameter of a levitated droplet is as large as 2–3 mm, by combining the levitation method with a brilliant synchrotron radiation or strong neutron source, many structural studies conducted by this method were reported.<sup>1–4</sup> As no container suppresses seeds of nucleation, deep undercooling is achieved. The idea that deep undercooling in metallic liquids is correlated with the presence of locally stabilized icosahedral clusters was presented by Frank.<sup>5</sup> Such local clusters with the symmetry forbidden in crystalline structures were investigated for undercooled liquid alloys.<sup>3</sup> Recently, quantitative measurements of the time-dependent nucleation rate in a bulk metallic glass have been combined with the measurements of the evolution of a supercooled liquid structure to a structure near the glass transition temperature, which confirms that icosahedral-order-based frustration is strongly associated with the glass transition in Zr-based glasses.<sup>6</sup>

As evidence of the icosahedral cluster was found even in monatomic liquid transition metals,<sup>4</sup> it may be helpful to study details of a local atomic configuration in liquid transition metals for deep understanding of the glass transition in bulk metallic glasses. Among the transition metals, iron is a common element in our life and a main component of the earth core. To understand liquid iron in the core under extremely high-temperature and high-pressure conditions inaccessible by experiments, a first-principles molecular-dynamics (MD) simulation has been carried out.<sup>7</sup> A reliable *ab initio* MD simulation for transition metals having d electrons with a localized character is now possible owing to recent developments of the methods based on the density-functional theory, such as a projector-augmented wave method.<sup>8</sup> However, very few *ab initio* MD simulations have been reported for liquid iron under ambient conditions.<sup>9</sup> This may partly be because the structure factor  $S(Q)$  of liquid iron above the melting temperature previously obtained by x-ray scattering<sup>10</sup> does not exhibit a fine structure in the second maximum although recent neutron-scattering results of levitating liquid iron<sup>4</sup> exhibit such structure in the second maximum, indicating the icosahedral ordering.

In this context, it is of great interest to investigate the profile of  $S(Q)$  for normal bulk liquid iron again. We have carried out x-ray scattering measurements for liquid iron just above the melting temperature by an energy-dispersive method using synchrotron radiation. This method is essentially the same as that used for structural studies on expanded fluid mercury at high temperatures and pressures.<sup>11</sup> Our liquid iron data show a fine structure in the second maximum, as observed by the neutron scattering for levitating liquid iron.<sup>4</sup> Moreover, we analyzed the data by a reverse Monte Carlo (RMC) method<sup>12</sup> and the inverse method<sup>13</sup> to find the correlation between icosahedral ordering and interatomic interaction. In this report, we present the bond-orientational order and effective pair potential  $\phi(r)$  of liquid iron, both of which were deduced from  $S(Q)$  obtained, and estimate the fraction of nearly icosahedral configurations in a snapshot obtained by RMC simulation.

X-ray diffraction measurements for liquid iron were conducted with an energy-dispersive mode using synchrotron radiation at the beamline BL28B2/SPring-8 in Japan. The storage ring at SPring-8 was operated at 8 GeV with a 100 mA constant current mode (top-up mode) during the present experiments. White x-rays irradiating from a bending magnet and collimating to  $0.2 \times 0.2$  mm<sup>2</sup> using double slits were incident on the sample and the scattered x-rays were collimated with double slits and detected with a pure Ge solid-state detector. The level of the collimation of the present diffractometer is higher than that in the previous experiments using a single slit for scattered x rays.<sup>11</sup>

The experiments for liquid iron were performed at 1843 K and at approximately 10 MPa using an internally heated high-pressure vessel made of an ultrahigh-tension steel, which permits a measurements up to 196 MPa. The vessel has seven Be windows for the scattered x-ray beams, which are located at the scattering angles ( $2\theta$ ) of 4, 7, 11.5, 15, 20, 25, and 33°, to cover a sufficiently wide scattering vector modulus range,  $Q$ , ( $Q=4\pi E \sin \theta/hc$ , where  $h$  is Planck's constant,  $c$  is the light velocity and  $E$  is the x-ray energy). The construction of the high-pressure vessel is shown in Ref. 14. In this experiment, the vessel was pressurized using He gas of high-purity grade (99.999%) to prevent hot iron from oxidation.

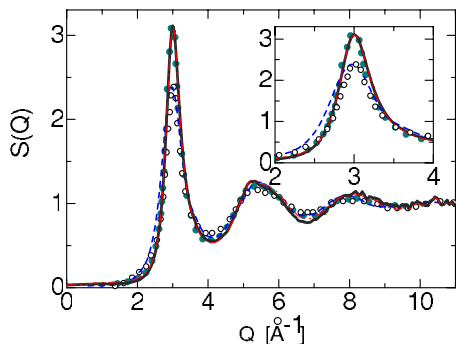


FIG. 1. (Color online)  $S(Q)$  (solid line) of liquid iron at 1843 K.  $S_W(Q)$  (Ref. 10) and  $S_N(Q)$  (Ref. 4) are denoted by a broken line and open circles, respectively. A chain curve denotes  $S(Q)$  deduced by RMC fitting.  $S(Q)$  at 1800 K reported by Ganesh and Widom (Ref. 9) is indicated by dots. The inset shows the first peak on an enlarged scale.

Using a sapphire cell that is slightly modified from the original Tamura-type cell,<sup>15</sup> we can prepare a stable thin slab of liquid transition metals. The cell was successfully applied to inelastic x-ray scattering experiments for liquid nickel<sup>16</sup> and liquid iron.<sup>17</sup> The hot part was heated using a tungsten heater surrounding a molybdenum tube. The temperature of the sample was measured using two W-5%Re:W-26%Re thermocouples. We prepared a cell with a sample space of 0.2 mm thickness for an appropriate x-ray transmission and inserted an iron sheet (99.998% purity) as the sample. The background was measured using another empty cell. In this experiment, however, as the sample space was not completely filled with liquid iron, the background was measured again using an empty part of the cell exactly under the same experimental conditions at 1843 K and approximately 10 MPa.

Figure 1 shows the  $S(Q)$  of liquid iron at 1843 K,  $S_W(Q)$  at 1833 K reported by Waseda,<sup>10</sup> and  $S_N(Q)$  at 1830 K obtained by neutron scattering and a levitation method.<sup>4</sup> As indicated in the inset, in comparison with  $S_W(Q)$ ,  $S_N(Q)$  exhibits the first peak as narrow as the present  $S(Q)$ , but the peak heights of  $S_N(Q)$  and  $S_W(Q)$  are similar. In our data, the peak width is more reliable than the peak height because the first peak was deduced from the spectrum at  $2\theta=7^\circ$ , indicating that the first peak width of  $S_W(Q)$  does not agree with these recent results. For the first peak height of the present  $S(Q)$ , uncertainties of several corrections during the data analysis for the energy-dispersive mode inevitably degrade its accuracy to  $\pm 5\%$ , as previously reported.<sup>11</sup> In the present study, the reliability of the peak height was confirmed as follows. We deduced a preliminary  $S(Q)$  in which the first peak height was approximately 2.8. However, the preliminary  $S(Q)$  could not be reproduced by RMC simulation. Furthermore, the iterations of MC simulations for deducing  $\phi(r)$  from  $S(Q)$  did not converge. Thus, we reanalyzed the data within the experimental accuracy and finally deduced the present  $S(Q)$  with the first peak being higher than that empirically known for liquids near the melting temperatures. In the present data,  $S(Q)$  at  $Q \leq 2 \text{ \AA}^{-1}$  was extrapolated to  $S(0)$ .

Another difference from  $S_W(Q)$  is that the present  $S(Q)$  exhibits an enhanced shoulder at  $6 \text{ \AA}^{-1}$  in the second maxi-

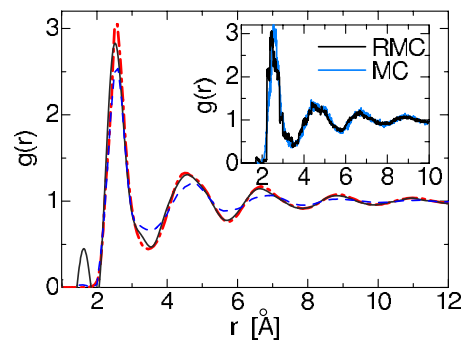


FIG. 2. (Color online)  $g(r)$  (solid line) of liquid iron at 1843 K. The broken and chain curves respectively denote the  $g(r)$  previously reported (Ref. 10) and that obtained by MC simulation using  $\phi(r)$ . The inset shows the radial distributions of a snapshot obtained by RMC and MC simulations.

mum, which has been discussed as evidence of icosahedral clusters in an undercooled liquid state. While these differences between the present  $S(Q)$  and  $S_W(Q)$  are observed in liquid iron, the  $S(Q)$  of liquid copper measured in the same experiments is in good agreement with  $S_W(Q)$ .<sup>10</sup> Hence, we do not consider that the pressure of 10 MPa affects the profile of  $S(Q)$  observed. In addition, the result for liquid copper indicates that the difference between the present  $S(Q)$  and  $S_W(Q)$  in liquid iron does not come from the difference in the geometrical condition of the spectrometer between transmission and reflection from the free liquid surface. The present  $S(Q)$  reproduced by RMC simulation is in good agreement with that obtained by *ab initio* MD simulation by Ganesh and Widom,<sup>9</sup> as shown in Fig. 1. We are surprised at this consistency because we independently analyzed the data before finding their results.

The pair distribution function  $g(r)$  deduced from the Fourier transform of  $S(Q)$  is shown in Fig. 2. The first peak is located at approximately 2.52 Å and a clear first minimum is observed at 3.5 Å. In comparison with  $g(r)$  obtained from  $S_W(Q)$ , the first peak in the present  $g(r)$  is slightly higher and slightly shifted to a smaller distance, and the oscillations are persistent to larger  $r$  values. We integrated  $4\pi n^2 g(r)$  up to 3.0 Å, where  $n$  is the number density, and obtained the nearest-neighbor coordination number of approximately  $10.2 \pm 0.4$ , while it becomes  $13.3 \pm 0.4$  in the integration up to the first minimum of 3.5 Å.

We carried out an RMC simulation for the system of 8000 particles using a hard-sphere cutoff distance of 1.5 Å. The  $S(Q)$  obtained by RMC simulation is shown in Fig. 1. The RMC simulation well reproduces the experimental data except for a small difference around the second peak, and we obtained an atomic configuration consistent with the present  $S(Q)$ . The inset in Fig. 2 shows a radial distribution of a snapshot obtained by RMC simulation. The coordination number and bond angle distributions calculated using the cutoff distance  $r_{\text{cut}}=3 \text{ \AA}$  are shown in Fig. 3.

For investigating bond-orientational order of the fivefold symmetry, we calculated  $\hat{W}_6$  (Ref. 18) for local clusters.  $\hat{W}_6$  takes a minimum value of  $-0.169$  for a regular icosahedron. In an undercooled Lennard-Jones liquid, Nose and Yonezawa<sup>19</sup> reported that the average  $\hat{W}_6$  does not indicate

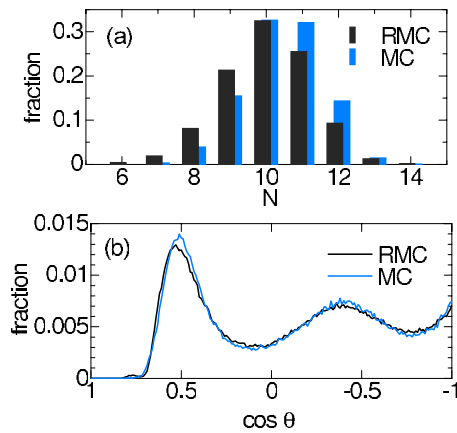


FIG. 3. (Color online) Distributions of coordination number (a) and bond angle (b) obtained by RMC and MC simulations using a cutoff distance of 3.0 Å.

clear evidence of the extensive fivefold symmetry. Here, we chose  $r_{\text{cut}}=3$  Å to define a local cluster and found that the average  $\hat{W}_6$  is  $-0.04235$ . We plot the distribution of  $\hat{W}_6$  in Fig. 4. The fraction of  $\hat{W}_6 \leq -0.13$ , indicating a value very near to the icosahedral limit,<sup>20</sup> is approximately 2%, while the fraction of  $\hat{W}_6 \leq -0.09$ , indicating a value of nearly icosahedral configurations,<sup>20</sup> is approximately 14%. These results indicate that the atomic configuration in liquid Fe shows a trend of icosahedral ordering. There appears a nearly regular icosahedron in a snapshot obtained by the present RMC simulation, as shown in the inset in Fig. 4. The formation of a local icosahedral cluster is also speculated from the enhancement of the slow viscoelastic decay observed at a small  $Q$  observed by inelastic x-ray scattering for liquid iron.<sup>17</sup>

As observed in Fig. 4, the profile of this distribution seems consistent with that obtained by *ab initio* MD simulation.<sup>9</sup> More precisely, the fraction near  $\hat{W}_6 = -0.05$  is larger in the RMC simulation than in the *ab initio* MD simulation, while the fraction near  $\hat{W}_6 = -0.16$  exhibits an opposite tendency. This may be associated with the fact that RMC modeling produces the most random configuration consistent with  $S(Q)$ .

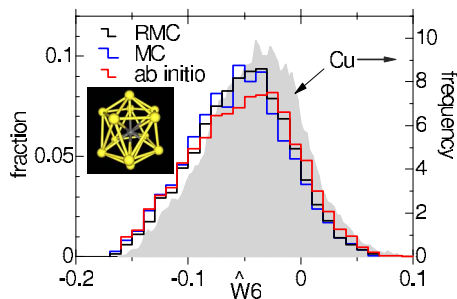


FIG. 4. (Color online)  $\hat{W}_6$  distributions obtained by RMC and MC simulations and that at 1900 K obtained by *ab initio* MD simulation (Ref. 9). Also shown is the frequency values (the right ordinate) of  $\hat{W}_6$  of liquid Cu (shaded area) obtained by RMC simulation (Ref. 20). The inset shows a snapshot of an icosahedral cluster in the RMC modeling of liquid iron.

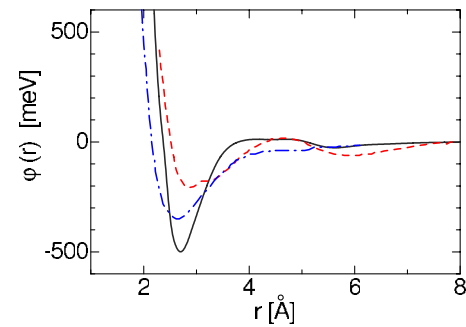


FIG. 5. (Color online)  $\phi(r)$  of liquid iron at 1843 K (solid line). A broken line denotes the  $\phi(r)$  reported by Kimmel and Gusenkov. Also shown is the  $\phi(r)$  reported by Hausleitner *et al.* (chain curve).

A similar RMC analysis was carried out for the x-ray scattering and x-ray absorption fine-structure spectra of undercooled liquid copper,<sup>20</sup> and a previously reported  $\hat{W}_6$  distribution in liquid copper is also shown in Fig. 4. The maximum position of liquid Cu slightly shifts to a larger  $\hat{W}_6$  and the fraction of  $\hat{W}_6 \leq -0.09$  in liquid copper is reported to be approximately 10%. Thus the present results for liquid iron indicate an enhanced icosahedral order compared with the ordering of liquid copper.

Now, we investigate why such icosahedral ordering appears in liquid iron above the melting temperature from the experimental data. A liquid metal consists of ions and conduction electrons, and the actual interaction between ions inside the metal should include many-body interaction. For deducing  $\phi(r)$  from  $S(Q)$  experimentally obtained, the inverse method with the predictor-corrector iteration proposed by Reatto *et al.*<sup>13</sup> may be the most sophisticated method at present, and this method has been applied to deduce  $\phi(r)$  for several types of liquid metal.<sup>21–23</sup> We deduced  $\phi(r)$  from the present  $S(Q)$  by this method using the bridge function, obtained by the modified hypernetted chain approximation<sup>24</sup> and the result is shown in Fig. 5. To realize self-consistency, we carried out an MC simulation at 1843 K using the  $\phi(r)$  for the system of 4096 particles in a periodically repeated cubic cell. As a result, the simulation reproduced  $g(r)$  within the experimental accuracy, as shown in Fig. 2 although a small shift of the first peak was observed. The atomic configuration obtained by MC simulation exhibits small differences from that obtained by RMC simulation in the radial distribution as well as the coordination number distribution, as observed in Figs. 2 and 3(a). However, the bond angle distributions are in excellent agreement with each other, as shown in Fig. 3(b). Consequently  $\hat{W}_6$  distributions for MC and RMC results almost agree with each other, as shown in Fig. 4.

Figure 5 also shows  $\phi(r)$  recently reported by Kimmel and Gusenkov,<sup>21</sup> who adopted the same inverse method using  $S_W(Q)$ . Similar results obtained using the same  $S_W(Q)$  have been reported.<sup>25,26</sup> These  $\phi(r)$  values exhibit a shallower minimum and stronger oscillations than the present  $\phi(r)$ . On the other hand, the attractive part in the present  $\phi(r)$  in Fig. 5 exhibits a deep minimum at 2.7 Å, which resembles the  $\phi(r)$  of iron reported by Hausleitner *et al.*<sup>27</sup> using a hybrid-

ized nearly-free-electron-tight-binding theory,<sup>28</sup> in which a covalent character of an unoccupied  $3d$  orbital in an iron atom is considered. The formation of the icosahedral cluster in liquid iron must be related to this deep minimum due to the unoccupied  $d$  states, while liquid copper, whose  $d$  orbitals are fully occupied, exhibits a weak icosahedral ordering, as was previously discussed.

Here, we estimate the total potential energies  $U$  of several clusters using the present  $\phi(r)$ . By assuming a bond distance of 2.5 Å, the  $U$  of a regular icosahedron is estimated to be approximately  $-18.0$  eV, while the  $U$  values of fcc and bcc clusters are determined to be  $-11.2$  and  $-17.3$  eV, respectively. As expected from the results of  $\hat{W}_6$  analysis, the regular icosahedron exhibits the most stable local atomic configuration among these clusters. Furthermore note that in the present estimation, the bcc cluster including 15 atoms seems as stable as the regular icosahedron compared with the fcc cluster. Ganesh and Widom<sup>9</sup> indicated how to induce icosahedral ordering in the liquid state from a bcc configuration. The stability of the bcc cluster in liquid iron near the melting temperature estimated from the present  $\phi(r)$  is consistent with the preference of the bcc structure in crystalline iron below the melting temperature.

In summary, the consistency of the present results with those obtained by the *ab initio* MD simulation reported by Ganesh and Widom<sup>9</sup> is encouraging and the present results suggest icosahedral ordering in liquid iron, as previously reported.<sup>4</sup> The fraction of nearly icosahedral configurations in liquid iron obtained by RMC simulation is approximately 14%, which is larger than approximately 10% reported for liquid copper.<sup>20</sup> The total potential energy of a regular ico-

hedron deduced from the present  $\phi(r)$  of liquid iron is slightly lower than that of a bcc cluster, while it is much lower than that of an fcc cluster. Although Ganesh and Widom have discussed icosahedral ordering in liquid iron and the preference of the bcc structure in the crystal based on their *ab initio* MD simulation results, the present results support their consideration from a classical potential picture based on the theory of simple liquids. Recently,  $S(Q)$  similar to that of liquid transition metals with icosahedral ordering has been reported from a structural study on charged colloidal liquids by Wette *et al.*<sup>29</sup> Because the charged colloidal liquids exhibit a soft repulsive potential with no attractive component, they have proposed that the softness of the repulsive part gives rise to the icosahedral ordering and the attractive part has secondary effects. Although their conclusion is very interesting, we cannot separate the effect of the soft repulsive part from the present  $\phi(r)$  exhibiting a deep attractive component. Instead the present analysis imply that the attractive interaction derived from unoccupied  $d$  orbitals plays a dominant role in the formation of local icosahedrons in liquid iron, as was presented by Frank.<sup>5</sup>

The authors would like to thank S. Hosokawa, K. Hoshino, S. Tanaka, and K. Kato for valuable discussion and A. Di Cicco for giving the numerical data of liquid copper. They would also like to thank the Ministry of Education, Culture, Sports, Science and Technology, Japan for a Grant-in-Aid for Scientific Research. The synchrotron radiation experiments were performed at the SPring-8 with the approval of the Japan Synchrotron Radiation Research Institute (JASRI) (Proposal No. 2008B1105).

- <sup>1</sup>H. Sinn, B. Glorieux, L. Hennet, A. Alatas, M. Hu, E. E. Alp, F. J. Bermejo, D. L. Price, and M.-L. Saboungi, *Science* **299**, 2047 (2003).
- <sup>2</sup>M. N. Greaves *et al.*, *Science* **322**, 566 (2008).
- <sup>3</sup>K. F. Kelton, G. W. Lee, A. K. Gangopadhyay, R. W. Hyers, T. J. Rathz, J. R. Rogers, M. B. Robinson, and D. S. Robinson, *Phys. Rev. Lett.* **90**, 195504 (2003).
- <sup>4</sup>T. Schenk, D. Holland-Moritz, V. Simonet, R. Bellissent, and D. M. Herlach, *Phys. Rev. Lett.* **89**, 075507 (2002).
- <sup>5</sup>F. C. Frank, *Proc. R. Soc. London, Ser. A* **215**, 43 (1952).
- <sup>6</sup>Y. T. Shen, T. H. Kim, A. K. Gangopadhyay, and K. F. Kelton, *Phys. Rev. Lett.* **102**, 057801 (2009).
- <sup>7</sup>D. Alfe, G. Kresse, and M. J. Gillan, *Phys. Rev. B* **61**, 132 (2000).
- <sup>8</sup>P. E. Blöchl, *Phys. Rev. B* **50**, 17953 (1994).
- <sup>9</sup>P. Ganesh and M. Widom, *Phys. Rev. B* **77**, 014205 (2008).
- <sup>10</sup>Y. Waseda, *The Structure of Non-crystalline Materials* (McGraw-Hill, New York, 1980).
- <sup>11</sup>M. Inui, X. Hong, and K. Tamura, *Phys. Rev. B* **68**, 094108 (2003).
- <sup>12</sup>R. L. McGreevy and L. Pusztai, *Mol. Simul.* **1**, 359 (1988).
- <sup>13</sup>L. Reatto, D. Levesque, and J. J. Weis, *Phys. Rev. A* **33**, 3451 (1986).
- <sup>14</sup>K. Tamura and M. Inui, *J. Phys.: Condens. Matter* **13**, R337 (2001).
- <sup>15</sup>K. Tamura, M. Inui, and S. Hosokawa, *Rev. Sci. Instrum.* **70**, 144 (1999).
- <sup>16</sup>S. Cazzato, T. Scopigno, S. Hosokawa, M. Inui, W. C. Pilgrim, and G. Ruocco, *J. Chem. Phys.* **128**, 234502 (2008).
- <sup>17</sup>S. Hosokawa, M. Inui, K. Matsuda, D. Ishikawa, and A. Q. R. Baron, *Phys. Rev. B* **77**, 174203 (2008).
- <sup>18</sup>P. J. Steinhardt, D. R. Nelson, and M. Ronchetti, *Phys. Rev. B* **28**, 784 (1983).
- <sup>19</sup>S. Nose and F. Yonezawa, *J. Chem. Phys.* **84**, 1803 (1986).
- <sup>20</sup>A. Di Cicco, A. Trapananti, S. Faggioni, and A. Filipponi, *Phys. Rev. Lett.* **91**, 135505 (2003).
- <sup>21</sup>A. Kimmel and I. Gusenkov, *Physica B* **382**, 257 (2006).
- <sup>22</sup>S. Munejiri, F. Shimojo, and K. Hoshino, *J. Phys.: Condens. Matter* **10**, 4963 (1998).
- <sup>23</sup>M. Inui, K. Matsuda, D. Ishikawa, K. Tamura, and Y. Ohishi, *Phys. Rev. Lett.* **98**, 185504 (2007).
- <sup>24</sup>Y. Rosenfeld and N. W. Ashcroft, *Phys. Rev. A* **20**, 1208 (1979).
- <sup>25</sup>T. Arai, I. Yokoyama, and Y. Waseda, *J. Non-Cryst. Solids* **106**, 104 (1988).
- <sup>26</sup>Y. Waseda and K. Suzuki, *Phys. Status Solidi B* **57**, 351 (1973).
- <sup>27</sup>C. Hausleitner, G. Kahl, and J. Hafner, *J. Phys.: Condens. Matter* **3**, 1589 (1991).
- <sup>28</sup>J. M. Wills and W. A. Harrison, *Phys. Rev. B* **28**, 4363 (1983).
- <sup>29</sup>P. Wette, I. Klassen, D. Holland-Moritz, T. Palberg, S. V. Roth, and D. M. Herlach, *Phys. Rev. E* **79**, 010501(R) (2009).